JOURNAL OF MATERIALS SCIENCE 23 (1988) 3903–3909

Miscible blends from rigid poly(vinyl chloride) and epoxidized natural rubber

Part 2 *Studies on mechanical properties and SEM fractographs*

K. T. VARUGHESE, G. B. NANDO, P. P. DE
Rubber Technology Centre, Indian Institute of Technology, Kharagpur 721 302, India
S. K. SANYAL
Department of Chemical Engineering, Jadavpur University, Calcutta 700 032, India

Mechanical properties and fracture of melt-blended poly(vinyl chloride) (PVC) and epoxidized natural rubber (ENR) having 50 mol % epoxidation level are studied at different compositions. The effect of blend ratio on tensile strength, tear strength, elongation at break, tension set after failure, and hardness are determined. The stress–strain behaviour of low ENR blends exhibits yielding and necking, whereas that of high ENR blends exhibits soft elastomeric deformation. At higher compositions of ENR, plots of tensile strength, tear strength, and hardness against blend composition are concave in nature; and plots of the elongation at break deviate markedly from the additive value with a pronounced maximum occurring at the 70 wt % composition of ENR. The scanning electron microscopic examination of fracture surfaces of blends does not show any features of phase separation of ENR or PVC. The tensile fracture surface of rigid PVC exhibits partially fused particle structures of PVC and that of blends exhibits features of shearing and horizontal discontinuous striations. The torn surface of rigid PVC shows evidence of intrinsic crazing and that of blends shows features of shear fibrils, vertically changed discontinuous striations, steps, and unstable and stable tear fronts.

1. Introduction

Blending of PVC with other polymers, which can function as plasticizers has gained considerable attention in recent years because the latter provide superior permanence in physical properties over their low molecular weight counterparts. It has been observed that blends of rigid PVC and ENR having 50 mol % epoxidation level form mutual miscible systems [1, 2] and ENR reduces the melt viscosity of rigid PVC [3]. Both melt-mixed [2] and solution-cast [1] blends have been reported to exhibit single glass–rubber transition temperatures (T_g) lying between those of ENR and PVC. In the present paper, we report the results of our studies on mechanical properties, such as stress–strain behaviour, tensile strength, elongation at break, tension set after failure, tear strength and hardness, and failure process. The fracture surfaces are examined by scanning electron microscopy (SEM) in order to understand the failure process.

2. Experimental procedure

Details of the materials used, formulations and mixing procedures are described in the previous paper [2]. The blends are denoted as P_{100}, P_{70}, P_{50}, P_{30} and P_0 corresponding to the weight percentage of rigid PVC. For instance, P_{70} represents 70/30 PVC/ENR and P_0 represents 0/100 PVC/ENR.

Tensile testing of the samples was done at

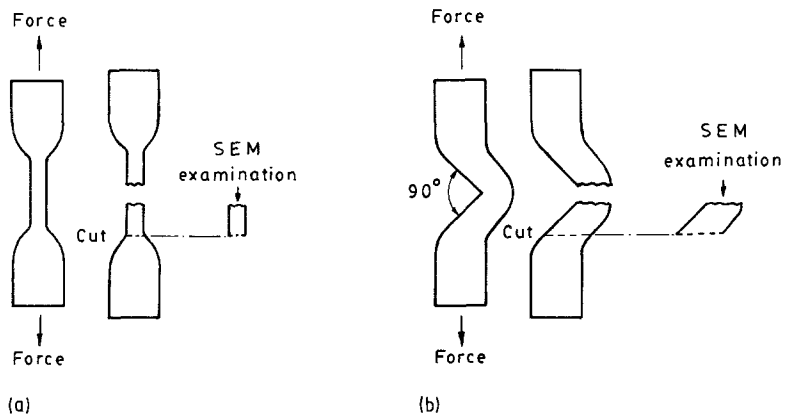

Figure 1 (a) Tensile and (b) tear test specimens showing fracture surfaces and area of SEM examination.

0022–2461/88 $03.00 + .12

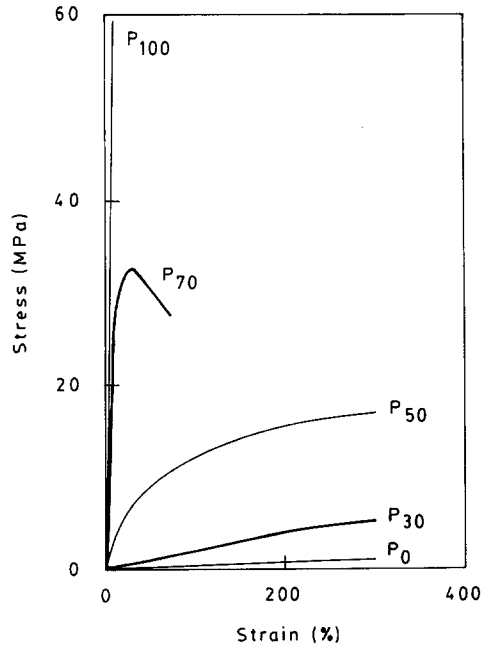

Figure 2 Stress–strain curves of PVC–ENR blends.

25 ± 2°C according to the ASTM D412-80 test method using a dumb-bell shaped test specimen in an Instron Universal Testing Machine (model 1195) at a cross-head speed of 500 mm min^{-1}. Tear strength of the sample was determined according to the ASTM D624-81 test using unnicked 90° angle test specimens. The tear test was carried out at the same conditions of temperature and cross-head speed as in the case of tensile testing. The tension set after break of the sample was measured according to ASTM D412-80. The hardness of the samples was determined and expressed in Shore D units.

The fracture surface of tensile and tear specimens were sputter coated with gold immediately after testing and SEM observations were made using Philips 500 model scanning electron microscope and the fractographs were taken along the direction of the fracture propagation adjusting the tilt angle to 33° in all cases. Fig. 1 shows the details of the test specimen,

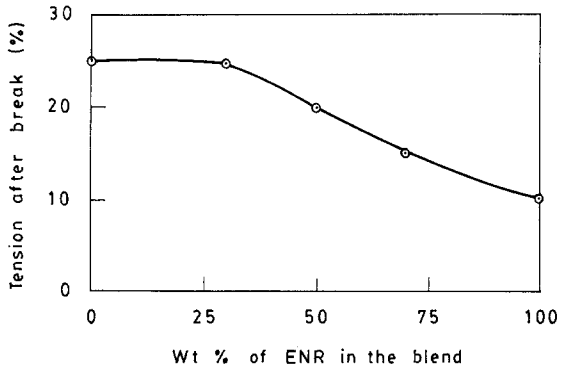

Figure 4 Effect of blend ratio on the tension set after failure of PVC–ENR blends.

fracture surfaces and the area of SEM examination in tensile and tear specimens.

3. Results and discussion

3.1. Stress–strain behaviour

The difference in deformation characteristics of samples under the uniaxial tensile stress is depicted in their stress–strain curves (Fig. 2). PVC (P_{100}) appears to have undergone a reversible deformation with the failure occurring at 10% strain. This indicates a brittle mode of failure in rigid PVC. ENR (P_0) exhibits the viscoelastic deformation of a very soft rubber and breaks at high strain.

Blends of rigid PVC and ENR show stress–strain behaviour ranging from the rigid response of PVC to the soft elastomeric nature of unvulcanized ENR. The deformation and the final rupture of P_{70} takes place in three steps.

(a) First is a linear viscoelastic deformation, where energy is stored in a quite reversible manner, extending the strain up to 10%.

(b) Second, is the anelastic region between 10 to 30% strain. At 30% strain, the yield point corresponding to the stress, 32.5 MPa is noted. The major failure event involved in this region is the formation of microshear bands before the yield point and macroshear bands at the yield point as reported by Richter

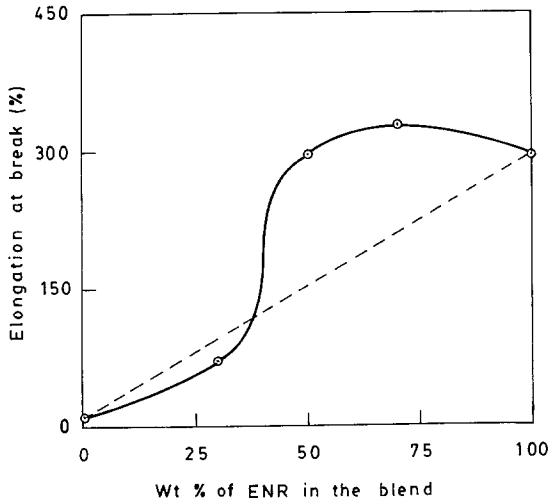

Figure 3 Effect of blend ratio on the elongation at break of PVC–ENR blends.

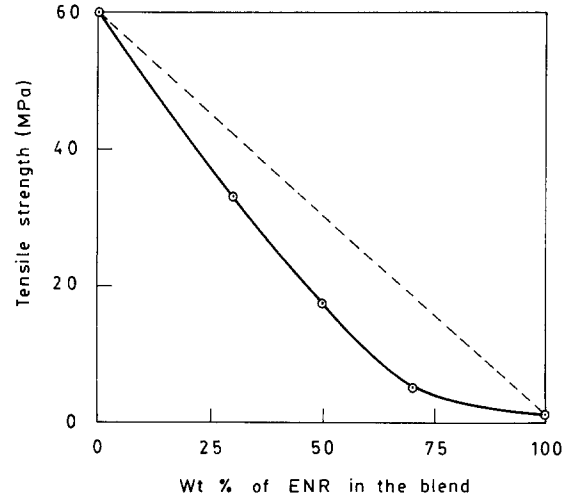

Figure 5 Effect of blend ratio on maximum tensile strength of PVC–ENR blends.

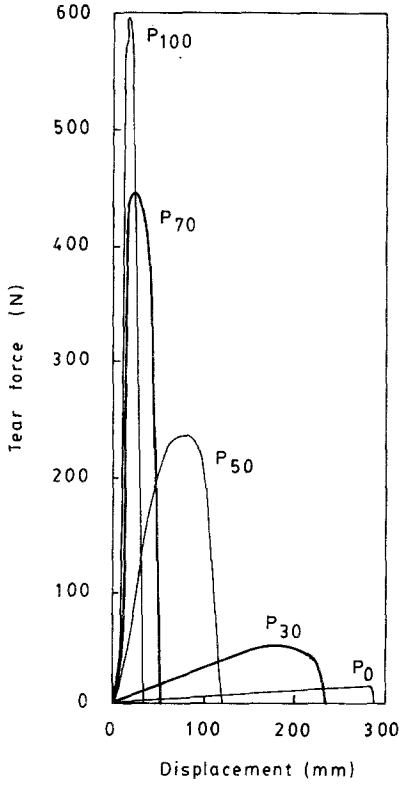

Figure 6 Tear force–displacement curves of PVC–ENR blends.

and Goldbach [4] for the deformation behaviour of PVC. Although crazing may also occur together with the shear banding process, it will be less prominent as understood for other rubber-modified PVC systems [5, 6].

(c) The third step is the necking deformation, beyond the yield point, accompanied by a fall in the stress until the final rupture. This indicates the onset of a large-scale viscous or plastic deformation of molecular coils.

At high levels of ENR, the yielding and necking disappear. P_{50} and P_{30} show rubber-like deformation as is often observed in plasticized PVC systems or soft elastomers. The dependence of stress–strain behaviour on blend ratio could be understood from the morphology and the difference in size of the interphase regions. In low ENR composition, ENR has only a minor contribution to the interphase size compared to the hard glassy blocks of PVC, whereas in high ENR composition, the interphase size is dominated by ENR which, because of its low modulus, converts the blend

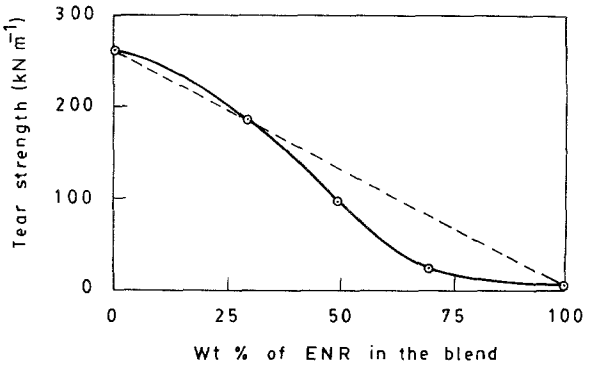

Figure 7 Effect of blend ratio on tear strength of PVC–ENR blends.

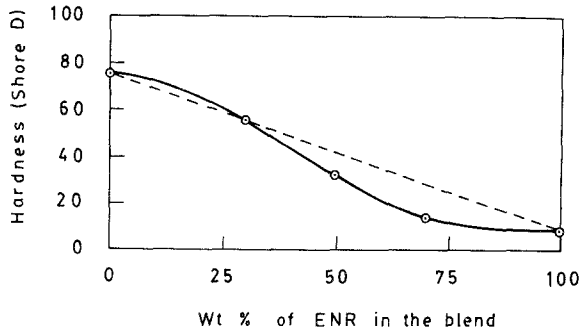

Figure 8 Effect of blend ratio on hardness of PVC–ENR blends.

into soft elastomeric solid. Consequently, viscous deformation of yielding and necking is suppressed in high ENR compositions leading to the final rupture through large rubber-like deformation.

3.2. Effect of blend ratio on properties

In blends, effect of composition on properties and deviation of properties from additivity have been discussed [7]. The effects of composition on properties of PVC–ENR blends are shown in Figs 3 to 8. For convenience, additive properties, wherever necessary, are indicated by dashed lines, which is derived from the equation

$$P = W_1P_1 + W_2P_2 \quad (1)$$

where W represents weight fraction of the polymer 1 or 2 and P, the property under consideration.

As shown in Fig. 3, the elongation at break, which is a strain-activated mechanical property, exhibits an exponential rise up to 40 wt % composition of ENR. This is then followed by a marked deviation from additivity with a pronounced maximum occurring at the 70 wt % composition of ENR. This deviation indicates extensive molecular mobility caused by the plasticization of rigid PVC by ENR in blends.

The effect of blend ratio on tension set after failure, which is a measure of permanent deformation, is depicted in Fig. 4. Macroscopically, the addition of ENR has little effect up to 30 wt % and thereafter a progressive decrease is noted up to 100 wt % ENR.

As shown in Fig. 5, the maximum tensile strength with respect to blend composition exhibits an improvement for ENR and a sharp reduction for PVC. The experimental values deviate from the additivity in a concave manner beyond 50 wt % composition of ENR.

Figs 6 and 7 show the tear force–displacement curves and tear strength against blend composition plot, respectively. As shown in Fig. 6, P_{100} tears at the smallest displacement and the highest force of all the samples. Unlike stress–strain behaviour, P_{100} in the tear force–displacement curve, on closer examination, exhibits yielding and plastic deformation. At a force of 570 N, the yield point is followed by plastic deformation up to final rupture at 600 N. The results of this plastic deformation are understood as intrinsic crazes from the fractographic studies of this paper. P_0 undergoes the largest displacement with the minimum tearing force. In P_{70}, the influence of the rigid response of PVC is evident from its small displacement and high

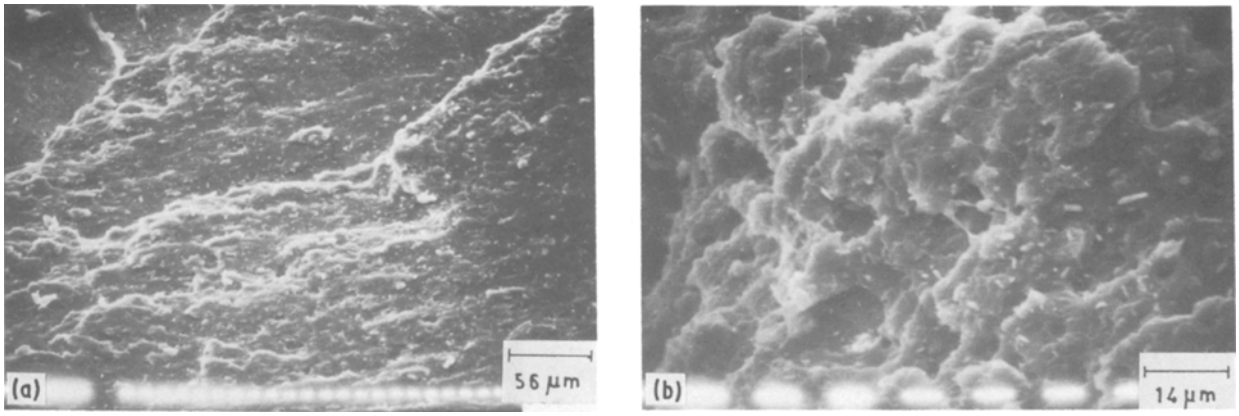

Figure 9 SEM of the tensile fracture surfaces of P_{100}: (a) low magnification, (b) high magnification, showing partially fused particle structures of PVC.

tearing force. As noted earlier in the stress–strain behaviour, the high level of ENR in the blend results in soft elastomeric deformation in the tear force–displacement as well. The area under the curve, which is maximum for P_{50}, indicates the highest energy expended for tearing of all the samples.

The effect of tear strength on blend composition is shown in Fig. 7. It is seen that the experimental plot passes above the additive plot beyond 70 wt % composition of PVC in the blend. This suggests tear deviation attributed to the physical networks existing between PVC and ENR in the high PVC blends. The nature of the tear strength plot at high ENR compositions of blends has a close similarity to that of tensile strength.

Variation of hardness of the samples with respect to blend composition is shown in Fig. 8. The nature of the plot exhibits a close similarity with the plot of tear strength at all blend compositions. Considerable upward deviation from additivity is noted up to 30 wt % of ENR followed by a progressive descent with a concavity at the high contents of ENR in the blend.

The formation of concavity at the high ENR compositions in plots of stress-activated properties such as tensile strength, tear strength and hardness appears to have an agreement with the T_g–blend composition plots of rigid PVC–ENR blends studied previously [2]. Interestingly, corresponding to the concavity for the aforementioned stress-activated properties, an upward curvature is noted in the elongation at break. The latter is a strain-activated mechanical property. These results corroborate the mutual miscibility in the PVC–ENR system or the plasticization of rigid PVC by ENR.

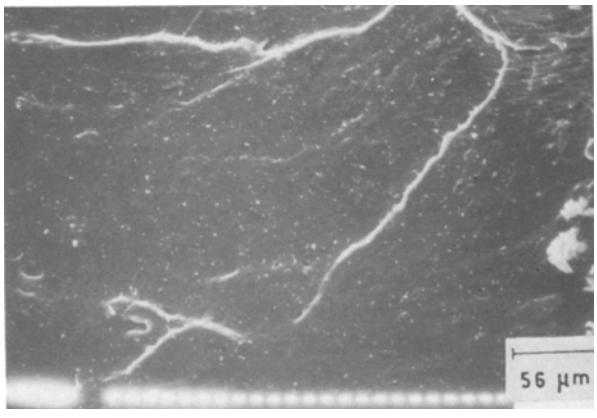

Figure 10 SEM of the tensile fracture surface of P_{70}.

3.3. Scanning electron micrographs

The study of the morphological features of the fracture surfaces using SEM is recognized as an important tool for understanding the cause of crack initiation and failure process in polymeric materials [8–13]. Fracture surfaces of dumb-bell shaped tensile and 90° angle unnicked tear specimens of PVC–ENR blends have been examined using SEM and the fractographs are shown in Figs 9 to 16. These two test specimens are different in geometry as is evident from Fig. 1. Hence, the effect of geometry (or type of testing) on fracture process is also depicted from the morphological features of the fracture surfaces of the respective test specimens. Moreover, none of the fracture surfaces exhibit features resulting from the separation of phases during failure.

3.3.1. Tensile failure

The first study concerning SEM of the tensile failure of rigid PVC was that of Cornes and Haward [14]. According to them, the crack front in the fracture surface originates and grows by tearing away the craze material at the pointed tips of a diamond cavity. Accordingly, a ductile failure occurs in rigid PVC prior to the plastic deformation. In a subsequent study, Lehtinen and Lindberg [15] reported diamond cavitation and the effect of cold flow in the injection-moulded rigid PVC. However, in the present study, the tensile failure of rigid PVC at the high strain rate appears to have occurred in a brittle manner, as is evident from the rough features of the fast fracture in both the low and high magnification SEMs. The brittle failure of rigid PVC is also proved from its stress–strain behaviour given in Fig. 2. In the high magnification SEM, partially fused particle aggregates of PVC are observed. Similar structural features in the SEM of PVC have also been noted by earlier investigators [16–18]. These particle aggregates act as physical networks and are responsible for higher strength in PVC. They are destroyed only by longer milling and for higher temperatures.

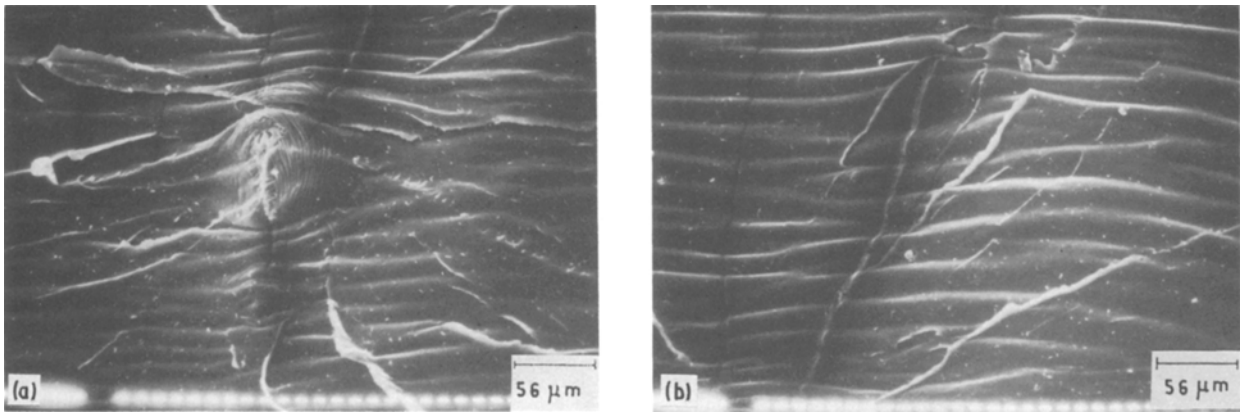

Figure 11 SEM of the tensile fracture surfaces of P_{50}: (a) internal flow and concentric shear rings; (b) another side of the fracture surface.

The SEM of P_{70} showing the fracture initiation site and the fracture propagation is given in Fig. 10. It is possible to see a smooth failure, which appears to have occurred from surface deformation, with the slow propagation of crack fronts characteristic of a single-phase ductile material. Several concentric rings present at the fracture initiation site are the indications of shearing deformation involved in the failure process. The effect of shearing of low ENR blend and the large soft elastomeric deformation of high ENR blend as demonstrated from the stress–strain behaviour is also depicted in the tensile fracture surface of rigid PVC–ENR blends. Horizontal discontinuous striations, which may result from the random orientations of the matrix along the stress axis and the subsequent incremental advancement of crack tip is evident in the fractograph of P_{50} and P_{30}. Figs 11a and 11b show such discontinuous striations of large deformation in P_{50}. In Fig. 11a, a stress-concentrated region of internal flow surrounded by concentric rings is noted. This suggests a certain extent of shearing involved during the fracture of P_{50}. P_{30} exhibits several irregular striations or foldings of a largely deformed fracture surface of very soft elastomers.

3.3.2. Tear failure

In tearing, the test specimen is subjected to a uniaxial tensile stress. The angular geometry of the tear specimen enables its apex to concentrate large amounts of stress and function like a notch. Hence, a triaxial stress [9] is produced at the apex of the angular region, which acts as a precursor for crack initiation. As the uniaxial stress is applied, failure initiates and propagates from the apex and allows more and more stress to concentrate at the tip of the advancing crack. Consequently, the particles nearby and along the crack paths at the fracture surface undergo large plastic deformation. In contrast to this, the dumb-bell geometry of the tensile test specimen makes its entire neck portion to have a more or less uniform stress distribution until the fracture develops from any of the growing cracks.

The fracture surface of the tear specimen of rigid PVC, P_{100} (Fig. 13), which has the highest strength of all the samples, exhibits microcavitations and fibrillar structures of intrinsic crazes, throughout the matrix. Similar features of microcavitations and fibrillar structures have been ascribed to intrinsic crazes by Kausch and co-workers (19–21) for the glassy polymers of polycarbonates and poly(methyl methacrylate). Stress-activated disentanglement of chains, either by chain slippage or by chain rupture plays an important role in the formation of intrinsic crazes [19–21]. The intrinsic crazing is also predicted from the plastic deformation as demonstrated in the tear force–displacement behaviour.

The torn surface of blends shows features that range from hard to soft polymers. The process of tearing involves the curving away of tear fronts, from the original plane of propagation, in an unstable manner.

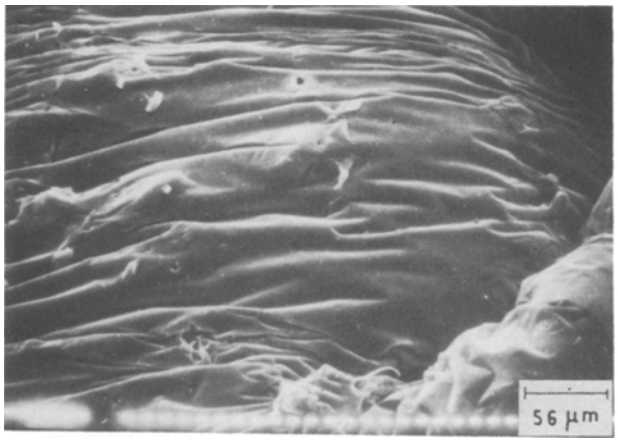

Figure 12 SEM of the tensile fracture surface of P_{30}.

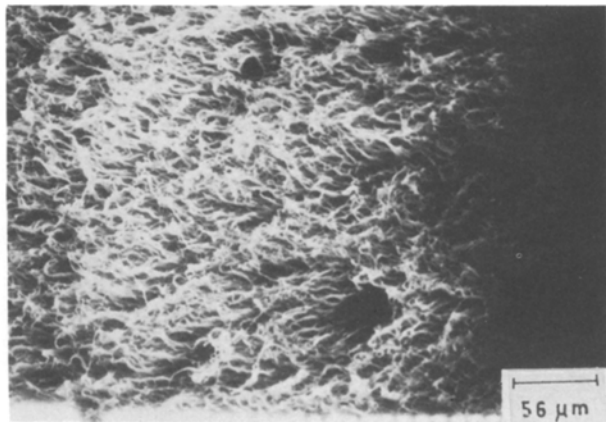

Figure 13 SEM of the tear fracture surface of P_{100}.

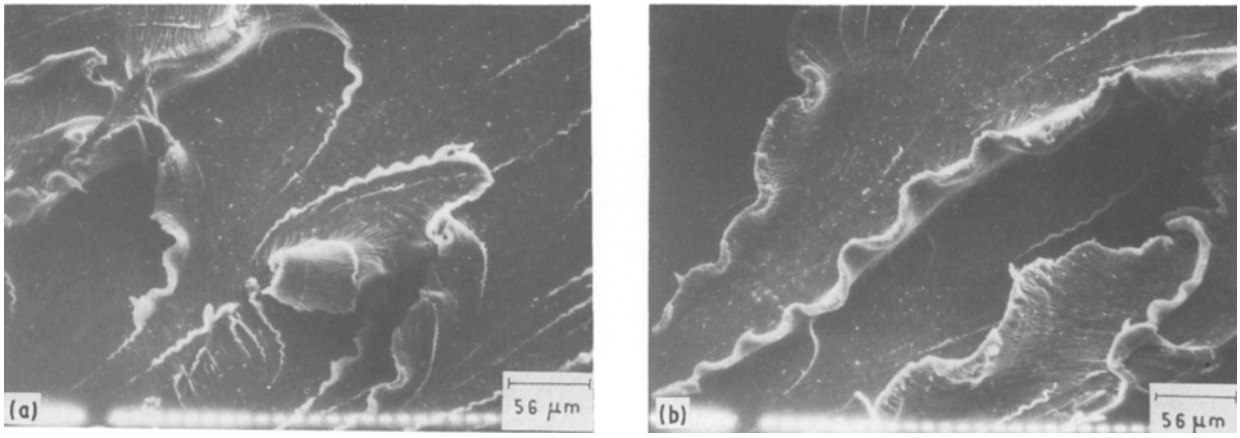

Figure 14 SEM of the tear fracture surface of P_{70}: (a) parabolic tear fronts and shear fibrils; (b) wavy tear paths and shear fibrils.

In P_{70}, (Figs 14a and b) because of the higher plastic deformation than other blends, the fracture surface exhibits features of several fine fibrils, parabolic and wavy tear fronts. The fine structure of fibrils gives an impression of extensive shearing together with crazing of the plastically deformed fracture surface. Hence, we observe these fibrils as shear fibrils, which could occur in the fracture surface of a glassy polyblend of PVC and ENR. Parabolic tear fronts in Fig. 14a are an indication of tear deviation, and the wavy tear paths represent the unstability of tear fronts due to crack blunting. It is proposed that the amount of localized plastic deformation that occurs at the crack tip prior to crack propagation is the controlling factor in crack blunting [22–23]. Frequent vertical striations at the matrix, with less unstable or damping wavy tear fronts, steady tear fronts, and steps are seen in the SEM fractograph of P_{50} (Fig. 15). Steps are noted as a characteristic feature of the torn surfaces of elastomeric materials [24]. In P_{30}, (Figs 16a and b) the large, elastomeric deformation results in a smooth ductile fracture surface with features of slightly distorted vertical striations of the matrix, steady tear path with diminished steps, and diminished parabolic tear fronts. From the SEM fractographs of the torn surfaces of rigid PVC–ENR blends, it is concluded that the blend having the higher tear strength exhibits maximum unstable tear fronts and as the strength is reduced by increasing the ENR level, a steady tear front is noted.

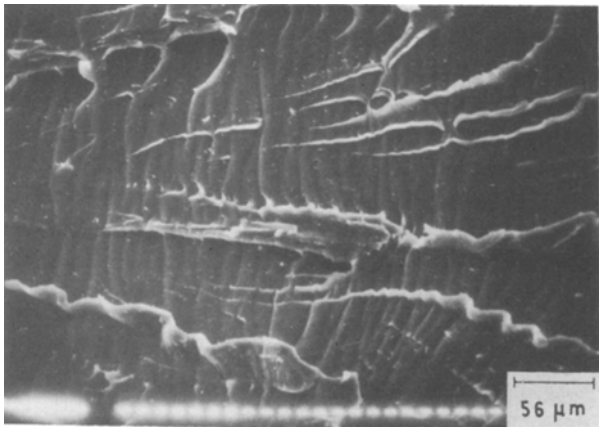

Figure 15 SEM of the tear fracture surface of P_{50}.

4. Conclusions

Flexibility of rigid PVC improves in blends with ENR. However, the stress-activated properties such as tensile strength, tear strength, and hardness decrease due to the soft elastomeric ENR. Results of stress–strain behaviour, tear force–displacement behaviour, and SEM of fracture surfaces corroborate a range of deformation extending from the rigid response of PVC to the unvulcanized elastomeric nature of ENR (in the blends). ENR delays the failure by shear yielding in low ENR blends and by soft elastomeric deformation in high ENR blends. The formation of concavity in plots of tensile strength, tear strength, and hardness appears to be similar to T_g–blend composition plots reported earlier [2]. The dumb-bell tensile specimen and the angular tear specimen produce features of different morphology in the respective SEM fractographs. This is attributed to differences in the fracture processes due to the difference in geometry of the test specimens (or the type of testing performed). Plastic deformation and intrinsic crazing is a characteristic feature of the angular (90°) tear specimens of rigid PVC that has failed under uniaxial tensile force. Shear fibrils, vertically changed discontinuous striations, steps, and the effect of blunting of crack tip are the major features of the torn surfaces of rigid PVC–ENR blends.

Acknowledgements

One of the authors (KTV) thanks Professor S. K. De for helpful suggestions and encouragement, and the Department of Science and Technology, New Delhi for sponsoring the research project.

References

1. A. G. MARGARITIS and N. K. KALFOGLOU, *Polymer* **28** (1987) 497.
2. K. T. VARUGHESE, G. B. NANDO, P. P. DE and S. K. DE, *J. Mater. Sci.* **23** (1988) 3894.
3. K. T. VARUGHESE, P. P. DE, G. B. NANDO and S. K. DE, *J. Vinyl Tech.* **9**(4) (1987) 160.
4. K. P. RICHTER and GOLDBACH, *Plast. Rubb. Process. Appl.* **6** (1986) 331.

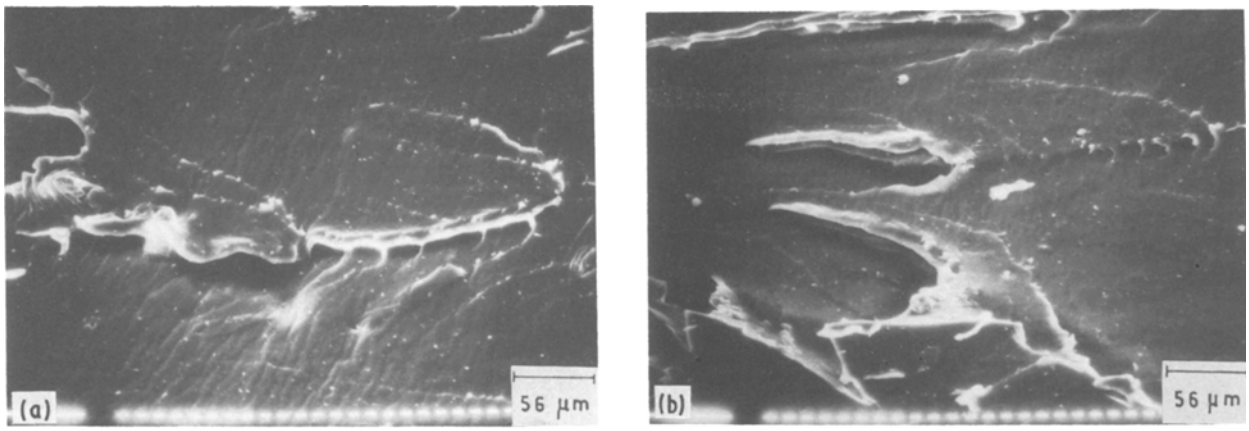

Figure 16 SEM of the tear fracture surface of P_{30}: (a) steady tear path and diminished steps; (b) diminished parabolic tear fronts.

5. H. BREUER, F. HAAF and J. STABENOW, *J. Macromol. Sci. Phys.* **B14** (1977) 387.
6. L. C. CESSNA, *Amer. Chem. Soc. Polym. Preprint* **15** (1974) 229.
7. H. SUAREZ, J. W. BARLOW and D. R. PAUL, *J. Appl. Polym. Sci.* **29** (1984) 3253.
8. H. H. KAUSCH, in "Polymer Fracture", Vol. 2 (Springer-Verlag, Berlin, Heidelberg, 1976) p. 200.
9. Y. FUKAHORI, *Int. J. Polm. Sci. Technol.* **9** (2) (1982) T/76.
10. *Idem, ibid.* **9** (8) (1982) T/58.
11. J. R. WHITE and E. L. THOMAS, *Rubb. Chem. Technol.* **57** (1984) 482.
12. S. S. BHAGAWAN, D. K. TRIPATHI and S. K. DE, *J. Mater. Sci. Lett.* **6** (1987) 157.
13. S. THOMAS, B. R. GUPTA and S. K. DE, *J. Vinyl Tech.* **9** (1987) 71.
14. P. L. CORNES and H. N. HAWARD, *Polymer* **15** (1974) 149.
15. T. S. LEHTINEN and J. J. LINDBERG, *J. Mater. Sci.* **11** (1976) 1764.
16. H. T. KAUW and F. E. FILISKO, *Macromol.* **12** (1979) 479.
17. J. W. SUMMERS and E. B. RABINOWITCH, *J. Macromol. Sci. Phys.* **B20** (1981) 219.
18. L. C. UITENHAM and P. H. GEIL, *ibid.* **B20** (1981) 593.
19. M. DETTENMAIER and H. H. KAUSCH, *Colloid Polym. Sci.* **259** (1981) 937.
20. *Idem, Polymer* **21** (1981) 1232.
21. A. DE BROSSIN, M. DETTENMAIER and H. H. KAUSCH, *Helv. Phys. Acta.* **55** (1982) 213.
22. R. A. GLEDHILL, A. J. KINLOCH and R. J. YOUNG, *Polymer* **19** (1978) 574.
23. R. A. GLEDHILL and A. J. KINLOCH, *Polym. Engng Sci.* **19** (1979) 82.
24. A. N. GENT and C. T. R. PULFORD, *J. Mater. Sci.* **19** (1984) 3612.

Received 5 November 1987
and accepted 1 March 1988